Hindawi
Journal of Nanomaterials
Volume 2022, Article ID 5722653, 11 pages
https://doi.org/10.1155/2022/5722653

Research Article

Wind Flow Simulation around Rhizophora Mangrove Roots Using Computational Fluid Dynamics

Sini Rahuman,[1] **A. Mohamed Ismail**,[1] **Shyla Manavalan Varghese**,[2] **George Kwamina Toworfe**,[3] **and Bashyam Sasikumar**[4]

[1]*Department of Mathematics, Sathyabama Institute of Science and Technology, Chennai, India*
[2]*Department of Developmental Mathematics, Houston Community College, Houston, Texas, USA*
[3]*Department of Engineering, Computing and Allied Sciences, Regent University College of Science and Technology, Ghana*
[4]*Faculty of Mechanical Engineering, Arba Minch University, Arba Minch, Ethiopia*

Correspondence should be addressed to Sini Rahuman; sini.rahuman@polytechnic.bh,
A. Mohamed Ismail; ismailbtl@yahoo.co.in, and Bashyam Sasikumar; bashyam.sasikumar@amu.edu.et

Received 19 March 2022; Revised 9 April 2022; Accepted 13 April 2022; Published 5 May 2022

Academic Editor: Samson Jerold Samuel Chelladurai

The characteristics of Rhizophora mangrove root structures and its efficiency in velocity dissipation process of heavy wind are studied in this paper. The influence of Rhizophora Mangrove roots on severe tropical storm (88 -117 km/hr.), intense tropical cyclone (166-212 km/hr.), and very intense tropical cyclone (above 212 km/hr.) is investigated by simulating wind flow around these roots with inlet velocities 100 km/hr., 200 km/hr., and 300 km/hr. ANSYS Fluent software is used for developing the computational fluid dynamic (CFD) model and to perform simulation and analysis. The flow velocity profile reveals that these mangrove root structures have a significant impact on the severe and intense wind flow. It is found that the Rhizophora root structures reduce the velocity of the wind by more than 80% of the inlet velocity. This information can be utilized to visualize and better understand the benefits of these root structures and to reestablish mangrove forest, create new breakwater models, and to strengthen the existing ones.

1. Introduction

Tsunamis, flooding, and mudslides are all natural disasters that have major influence on the ecosystems. Mangrove forests provide coastal protection, according to several studies. By using the results of the statistical tests, researchers have been able to analyze and calculate the efficiency of coastal vegetation in Japan against tsunamis [1]. After the tsunami of December 2004, another study was conducted in 18 coastal hamlets along India's southeast coast, emphasizing the relevance of mangrove trees in coastal region protection [2].

There must be sufficient densities of mangrove trees to lower the height of the wave, preserve balance in sedimentation process, limit the depth of the tsunami flood, and decrease waves and winds on surge top [3]. Mangrove forests help to minimize erosion and promote the formation of good soil. A healthy mangrove is required for all aspects of coastal defense. It is important to understand how mangrove roots play an important role in safeguarding the coastlines by dissipating inlet energy of the wave and providing an effective sediment trapping mechanism.

Many analytical researches have been undertaken to explore and determine the relevance of mangrove forest. The drag coefficient associated with various Reynolds numbers, as well as the change in the number of trunks and their diameters for various distances from the seabed are discussed and analyzed in [4]. Researchers introduced a linear mathematical model that can estimate the attenuation of wave energy in mangrove forests in [5]. The thesis [6] develops and analyzes a model of wave propagation across a nonuniform mangrove forest.

Researchers considered the bottom as an inclined bottom surface in research on a nonuniform forest with

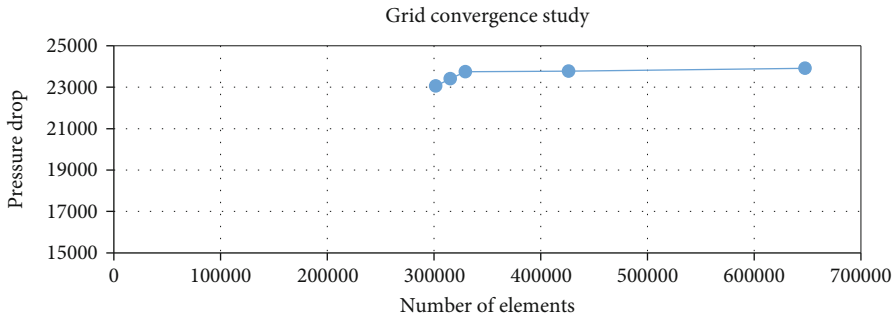

Figure 1: Grid convergence study.

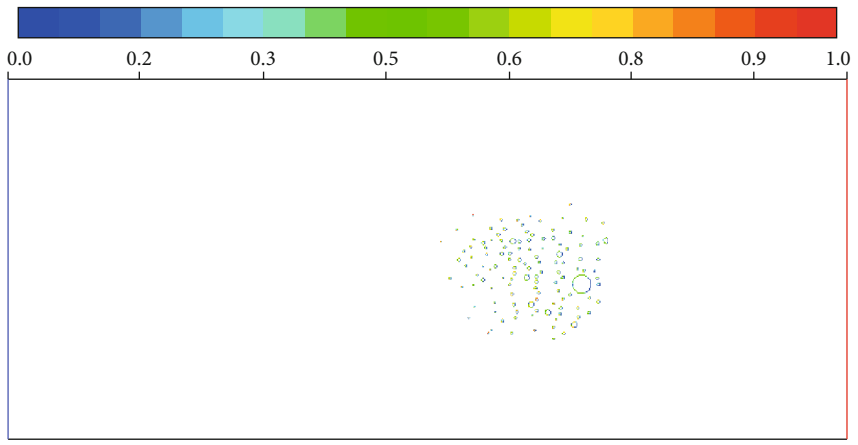

Figure 2: Wall $Y+$ of wall roots.

arbitrary depth [7]. The forest was represented as an array of vertical cylinders in a study by [8], which examined at the propagation of long surface waves across these forests. To explore wave attenuation across mangrove trees, a model was created and investigated a wave over a viscoelastic bed [9]. In [10], the influence of a thin viscoelastic mud layer on wave propagation across mangrove trees was investigated using linear theory. To measure bed friction and simulate turbulence caused by flow through tree trunks, simple models were used. Another study was performed computationally and experimentally to analyze the interaction of a solitary wave with emergent, rigid vegetation [11]. To examine turbulent mixing, surface wave attenuation, and nearshore circulation generated by vegetation, researchers constructed a nonhydrostatic RANS model. The bulk drag coefficient is the most important parameter affecting surface wave damping by plant canopies, according to their findings [12]. Numerical simulation of the effects of vegetation dampening on solitary water wave run-up is investigated in [13].

In recent years, numerical methods for predicting and reproducing the influence of mangrove forests on tsunami wave propagation have been developed. The majority of these numerical models are based on two-dimensional vertical averaged equations in shallow water. The Morison equation was introduced in [14]. For these coefficients, they employed the formulas presented in [15], which were based on data obtained in a Japanese coastal pine forest. The volume of trees under the water surface within a given control volume was used to quantify the formulations. In [16], researchers used the SWAN model to execute the research from [17], to simulate wave dissipation over vegetation areas. For vegetation with varied vertical area, such as mangroves, they included a vertical layer schematization. These models can be used to estimate the amount of wave damping produced by mangrove forests, but they rely on empirical coefficients that must be calibrated in order to yield meaningful results.

More recently, the Navier–Stokes (NS) equation used with the goal of improving the understanding of dissipation mechanisms is caused by vegetation [18]. The Navier–Stokes (NS) equation-based models were used to simulate flow vertical components as well as flow between individual elements while taking into account turbulence effects. Researchers in study [19] proposed a semianalytical theory of wave propagation across vegetated water based on a linearized version of the NS equations as a first approximation.

[20] studied sediment transport brought by tidal currents in mangrove forest. Mangrove forest reduces the forward speed of waves, resulting in a smaller flooded area [21]. [22] observed steady channel flow with uniform inlet flow velocity 0.2 m/s and flow in creeks with wave amplitude 1 m to study the blockage characteristics and the drag force of Mangroves. The above studies focused on the overall

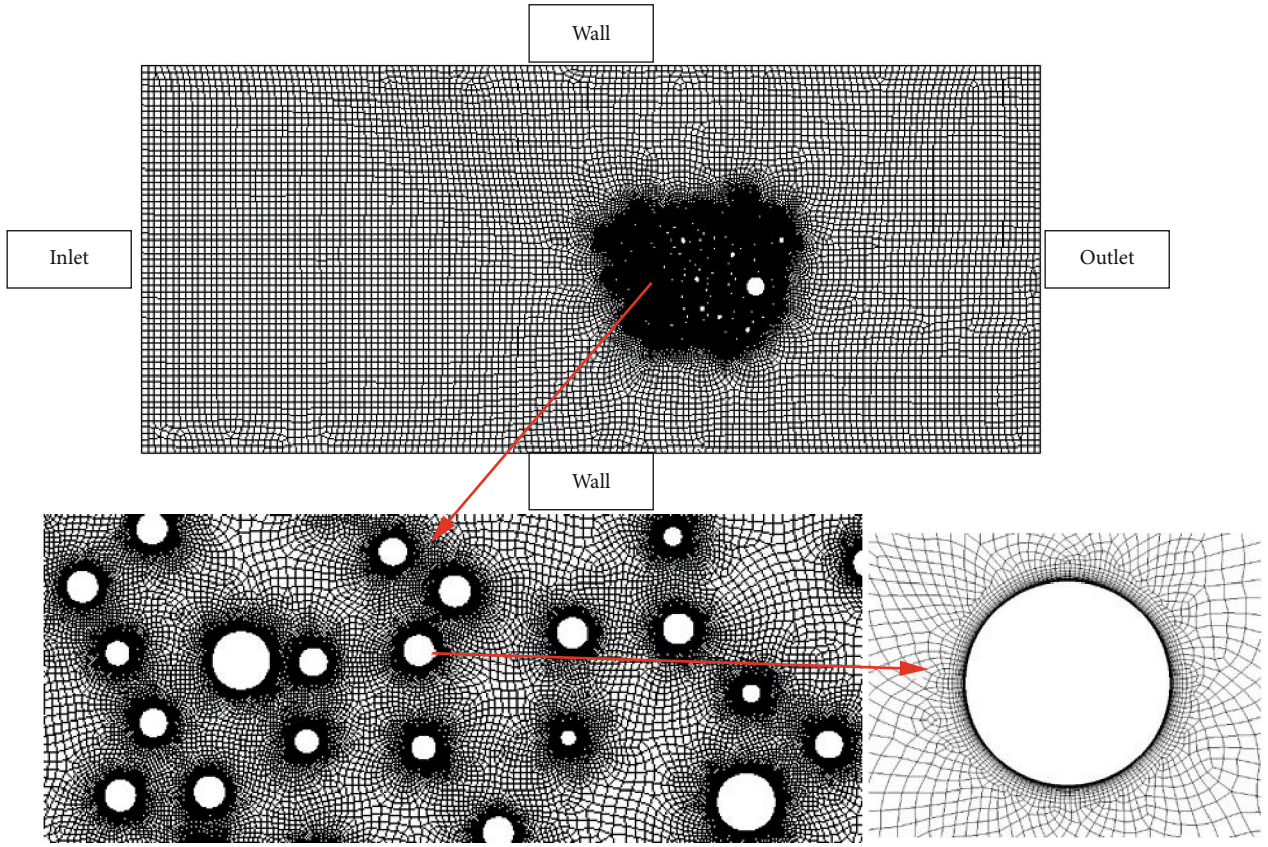

Figure 3: Mesh created in Ansys V 18.1.

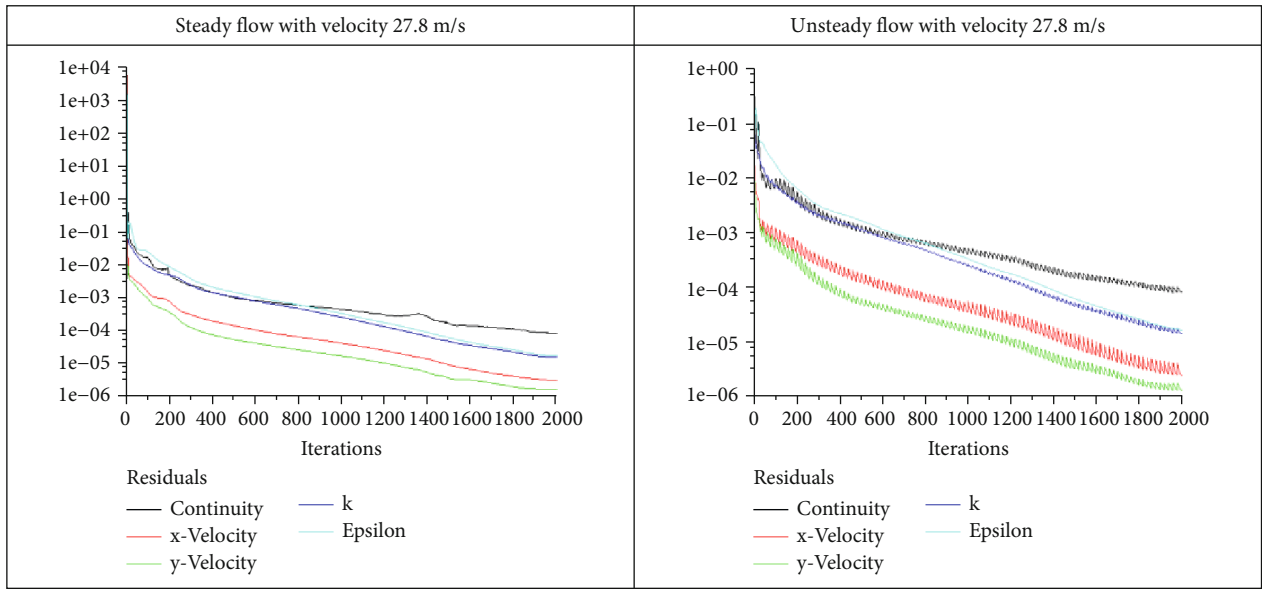

Figure 4: Steady and unsteady convergence plot of wind flow in case 1.

structure of Mangrove Forest rather than analyzing the individual species.

Mangrove roots are unique in that they include aerial roots that let plants grow firmly on muddy coastlines. The aerial root is capable of separating the salt content of water from pure water and allowing sedimentation to aid in the preservation of the mangrove habitat [23]. Different types of root development and aerial roots are adapted by different

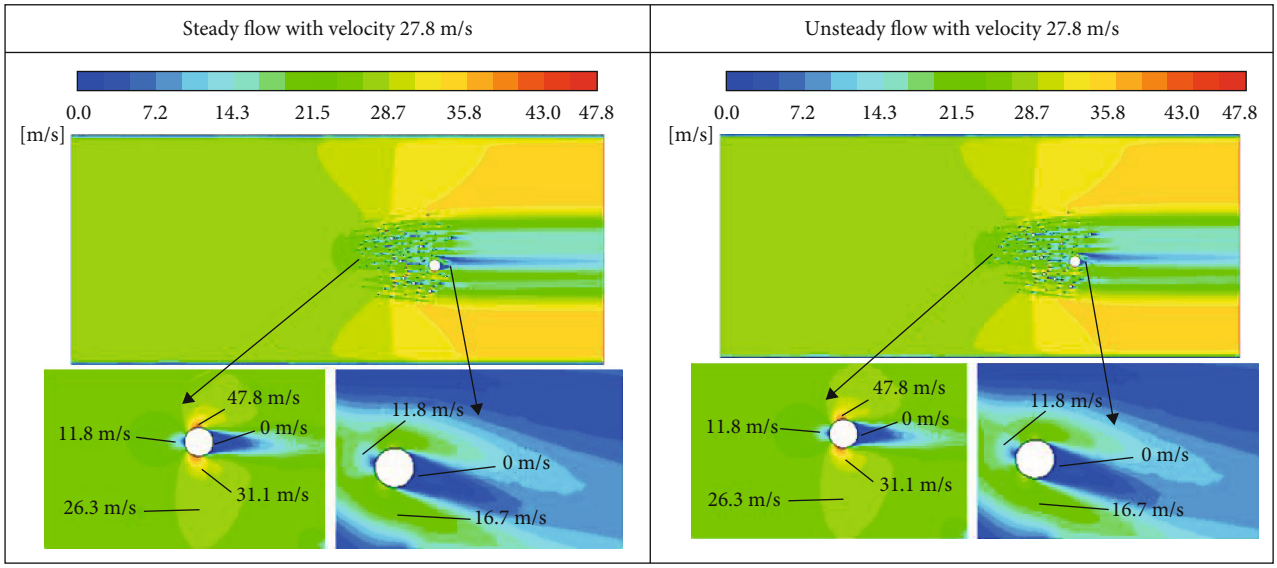

Figure 5: Steady and unsteady convergence plot of wind flow in case 2 steady flow with velocity 55.6 m/s.

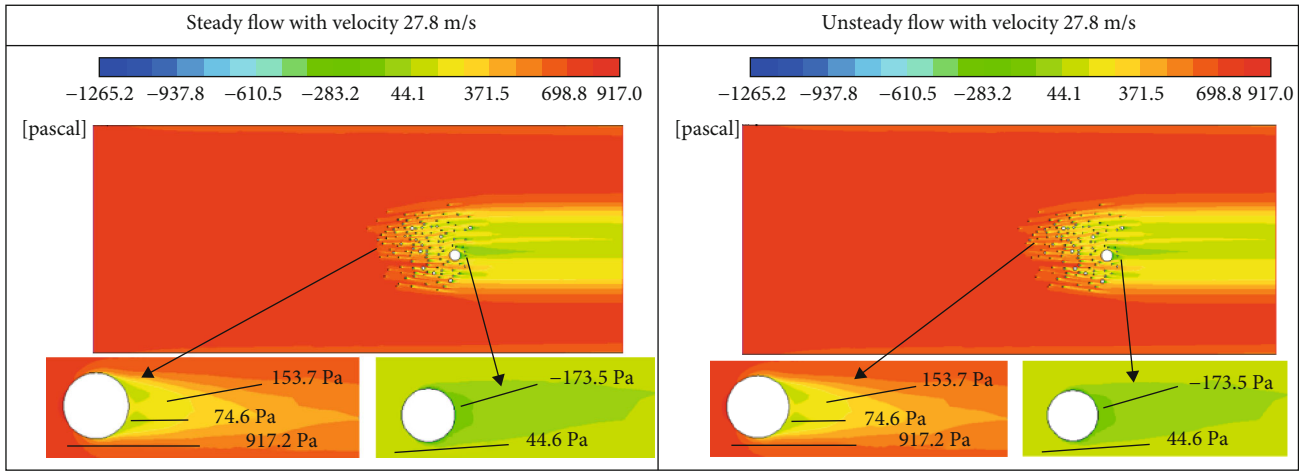

Figure 6: Steady and unsteady convergence plot of wind flow in case 3.

Mangrove species. Prop (stilt) roots, Pneumatophores, and knee roots are the three basic types of aerial roots. Prop roots are connected with Rhizophora, Pneumatophores with Avicennia, and knee roots with Bruguiera mangrove species [24]. The roots of mangrove trees serve an important function in lowering the tidal wave's force. The flow patterns within the root area were examined using two-dimensional water flow simulation around the Mangrove species Rhizophora apiculata and Avicennia marina [25].

Another study performed the water flow around mangrove species with inlet velocity as 6 m/s and analyzed the flow pattern around these roots [26]. Another CFD study performed to investigate the 2D water flow around the roots using different turbulence models and identify that the roots can reduce the water velocity [27]. CFD has been used to analyze wind flow (compressible and incompressible) around Avicenia mangrove roots to analyze the flow patterns around the roots [28]. Another CFD study conducted recently to investigate the water flow patterns around Rhizophora mangrove roots by using the velocity as step function, in which it was discovered that the root has the capacity of reducing the velocity of fluid [29].

Mangroves can also help lessen the effects of wind. Another quantitative analysis revealed that the land behind the Mangrove zone can be protected from category 5 typhoons with a fast forward speed of 11.2 m/s [30]. Wind flow around Avicenia mangrove roots was analyzed to study the characteristics of Pneumatophores in reducing the damages caused by heavy winds [30].

Very few studies have employed numerical techniques to analyze fluid flow around various media using computational fluid dynamics (CFD). CFD not only reduces the cost of experimental set up but also is reliable and efficient. Hence, this study uses computational fluid dynamics (CFD) in analyzing the behavior and efficiency of prop roots of Rhizophora mangrove species in reducing the wind flow

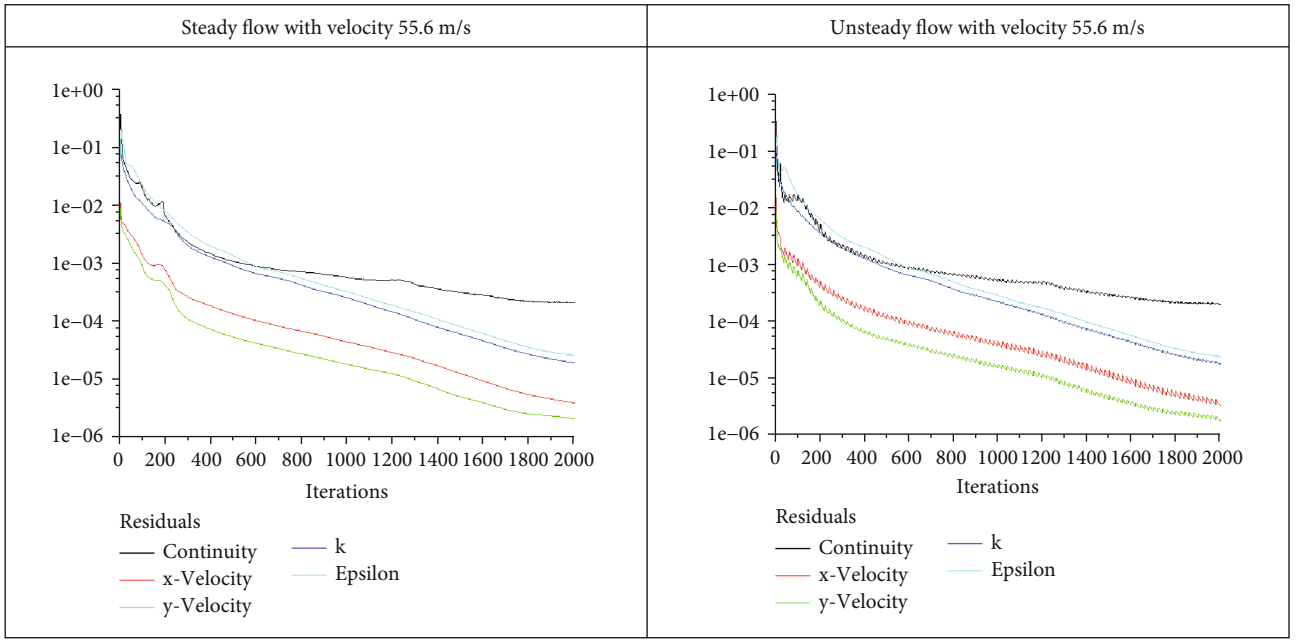

Figure 7: Steady and unsteady velocity contour of wind flow in case 1.

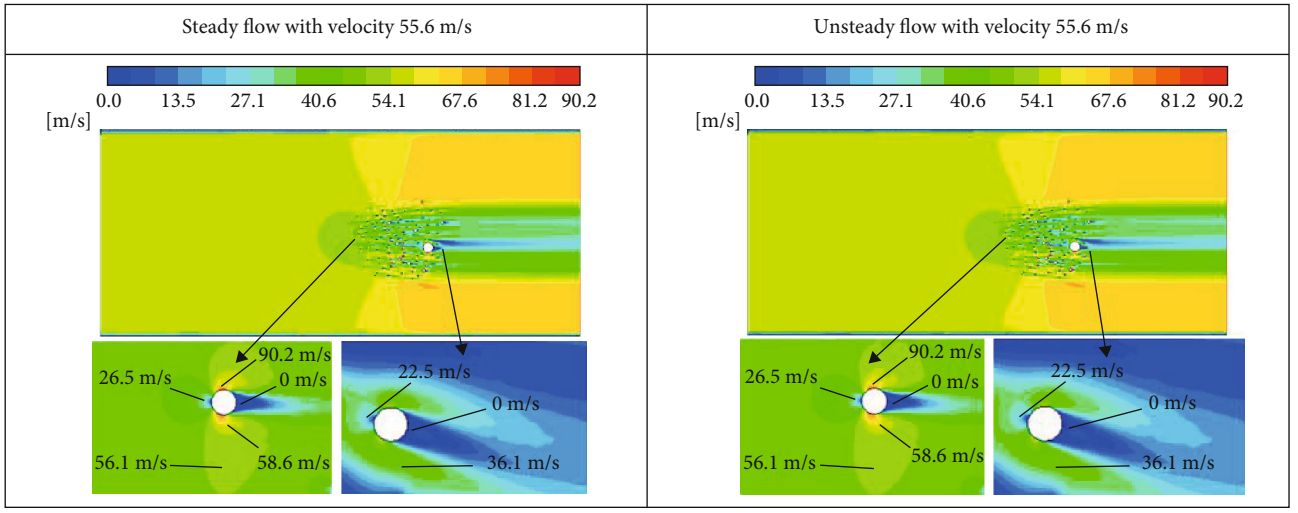

Figure 8: Steady and unsteady velocity contour of wind flow in case 2.

velocity during severe tropical storm (88 -117 km/hr.), intense tropical cyclone (166-212 km/hr.), and very intense tropical cyclone (above 212 km/hr.)

2. Methods

2.1. Study Approach. The steady and unsteady incompressible flow of wind around the roots of Rhizophora species is simulated using CFD and $k-\varepsilon$ turbulence model. The speed of wind during the severe tropical storm is considered as 100 km/hr. (steady and unsteady flow) at the inlet for case 1. The speed of wind during the intense tropical cyclone is considered as 200 km/hr. (steady and unsteady flow) at the inlet for case 2. The speed of wind during the very intense tropical cyclone is considered as 300 km/hr. (steady and unsteady flow) at the inlet for case 3. Finite volume method applied in this research to solve the problem.

2.2. Governing Differential Equation. Navier-Stoke's system of equations governing incompressible flow is as follows:

Continuity equation is as follows:

$$\nabla.\vec{q} = 0. \tag{1}$$

Momentum equation is as follows:

$$\rho\left(\frac{\partial\vec{q}}{\partial t} + \vec{q}.\nabla\vec{q}\right) = -\nabla p + \mu\nabla^2\vec{q}. \tag{2}$$

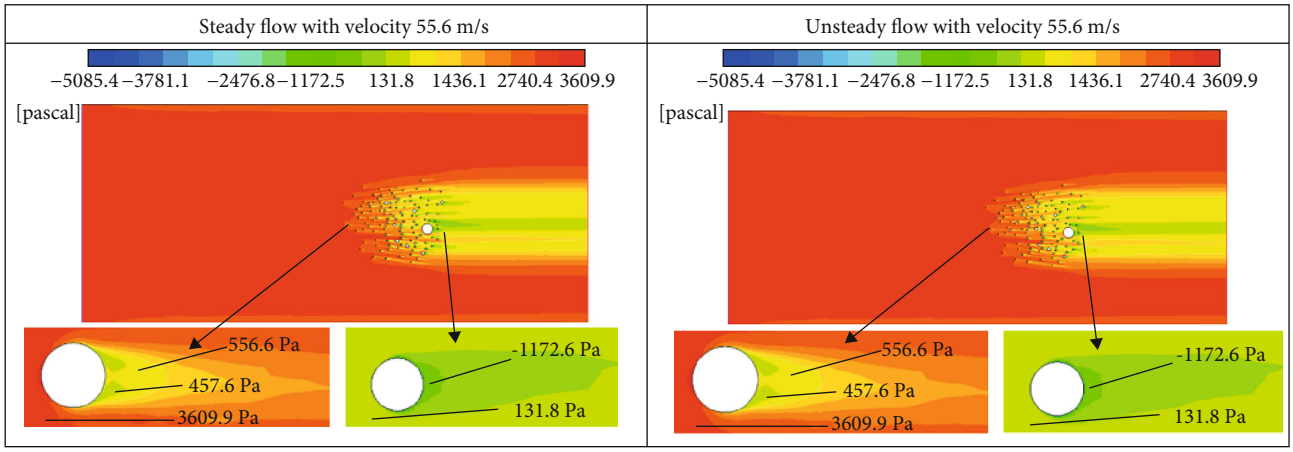

Figure 9: Steady and unsteady velocity contour of wind flow in case 3.

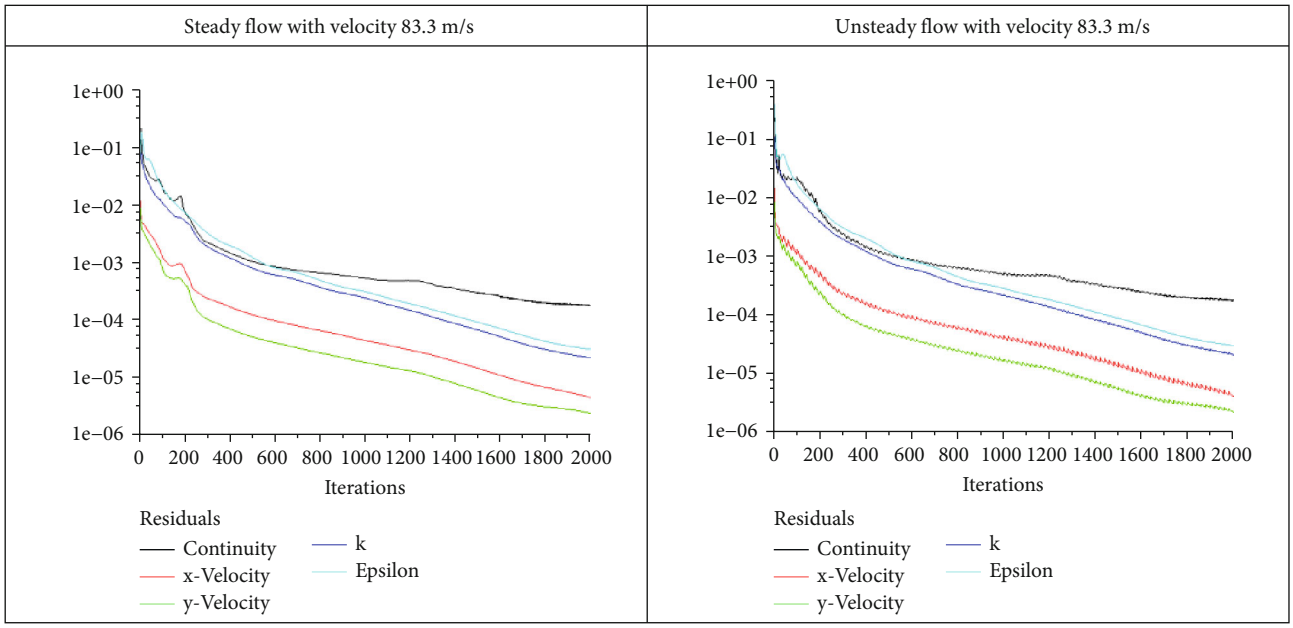

Figure 10: Steady and unsteady pressure distribution of wind flow in case 1.

2.3. Boundary Condition. Various inlet velocities are used to drive the simulation of two-dimensional air flow. The k-turbulence model is adopted in this research since the Reynolds number is more than 500000. The walls are fixed (no slip boundary condition), and the body forces are all ignored in this study. The outlet is designated as a pressure outlet, with a condition of 0 Pascal.

Case 1. Steady and unsteady wind flow with constant velocity 100 km/hr (27.8 m/s).

Case 2. Steady and unsteady wind flow with constant velocity 200 km/hr (55.6 m/s).

Case 3. Steady and unsteady wind flow with constant velocity 300 km/hr (83.3 m/s).

The mach number of all 3 cases is less than 0.3. So, the flow is considered as incompressible viscous flow.

The density of air $\rho = 1.225\,\text{kg/m}^3$ and the physical properties of air are used in this study with viscosity coefficient $\mu = 1.7894e^{-05}\,\text{kg/m}^{-}\text{s}$ that is applied in cases 1, 2 and 3. The pressure-based solver is used to solve this problem.

2.4. Methodology. The V-18.1 Ansys workbench design modeler was used to generate a computational model of the geometry with roots plotted in a 300 cm by 300 cm structure. To reduce the boundary effect on the air flow, a far field with an open boundary of 1500 cm by 700 cm is formed around the root geometry. Grid independent study performed with different mesh sizes to identify the suitable grid resolution for analysis of steady state. "Figure 1" represents the changes of pressure drops with number of elements. Based on the grid independent test, a mesh with 405012

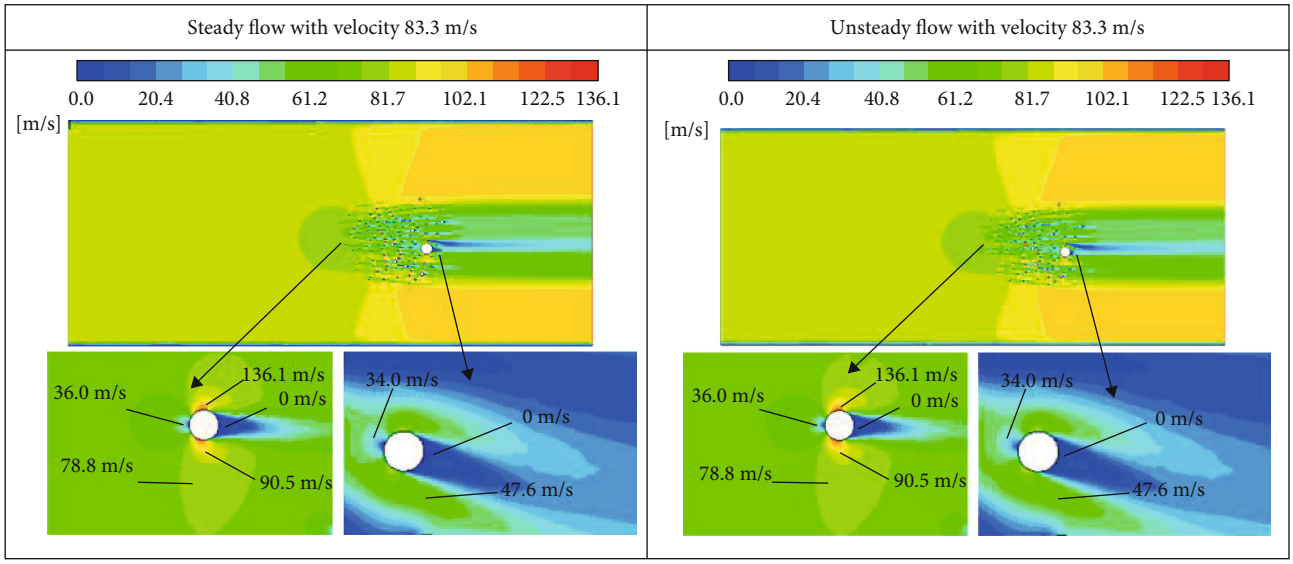

Figure 11: Steady and unsteady pressure distribution of wind flow in case 2.

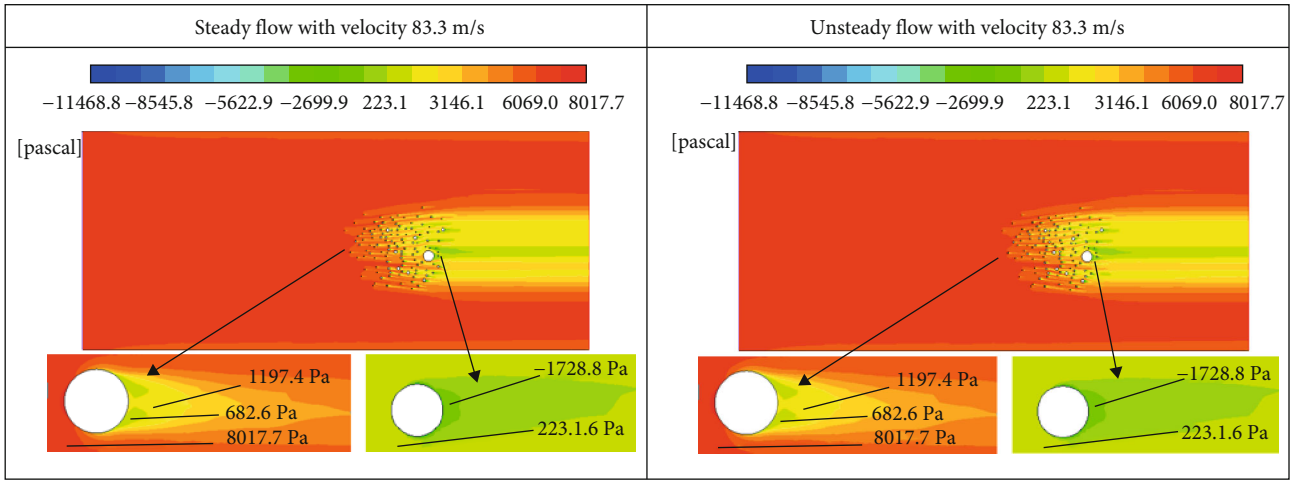

Figure 12: Steady and unsteady pressure distribution of wind flow in case 3.

cells, is used to perform the simulation of this study. Good quality mesh generated with wall $y+$ of wall root is approximately 1 that is shown in "Figure 2." The different sizes of primary prop roots are represented as big circle, and stilt roots are indicated as small circles are visualized in "Figure 3." Fine mesh is generated around the mangrove roots and which are clearly shown in the enlarged image of the roots in "Figure 3." Using the CFD program Ansys Fluent 18.1, the boundary is established, and the mesh is exported for CFD analysis.

3. Results and Analysis

Case 1. Steady and unsteady incompressible wind flow with constant inlet velocities 27.8 m/s(100 km/hr.).

Case 2. Steady and unsteady incompressible wind flow with constant inlet velocities.

Case 3. Steady and unsteady incompressible wind flow with constant inlet velocities 83.3 m/s (300 km/hr.)

Figures 4, 5, and 6 represent by steady and unsteady convergence plot of wind flow in cases 1, 2 and 3, respectively, which shows that the simulation convergence to three decimal places.

The comparison of steady and unsteady velocity contour of wind flow in cases 1, 2 and 3 is visualized in Figures 7, 8, and 9. The velocity contour of steady and unsteady wind flow in each case is same, which is clearly shown in these figures. The big white circle indicated by the main root and the small dots is represented by stilt roots of the Rhizophora tree. The roots have the capacity to reduce the wind flow to a great extent, which is clearly observed from these figures as different colors of contour (red is represented by very high velocity whereas blue represented be very low velocity). The enlarged images represented by two roots at different

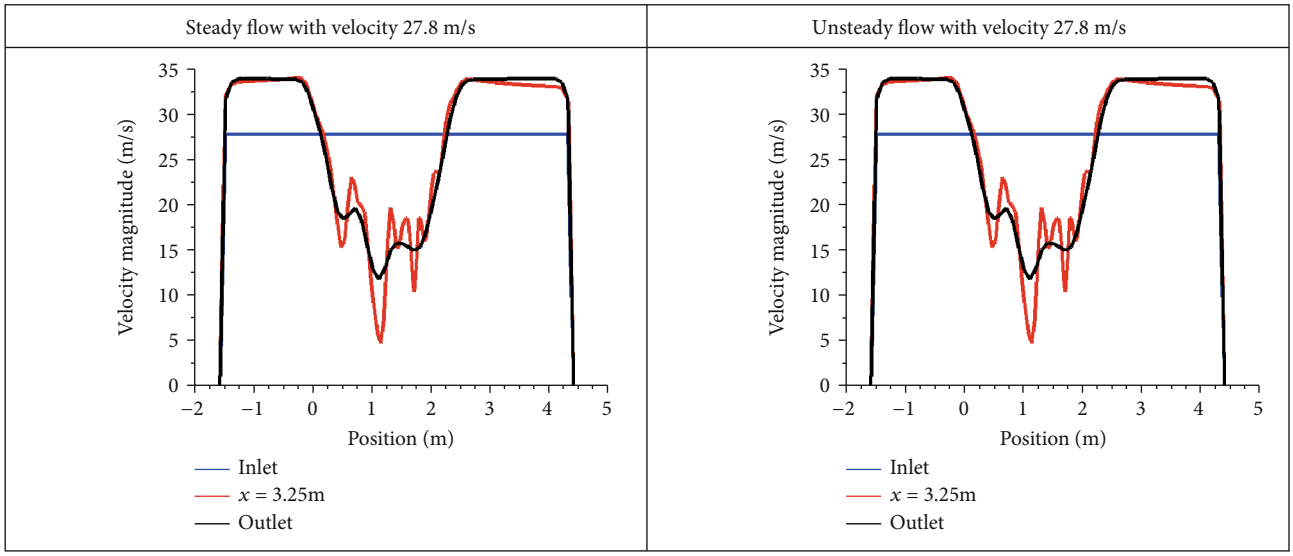

Figure 13: Steady and Unsteady velocity dissipation of wind flow at Inlet, outlet and x=3.25m in case 1.

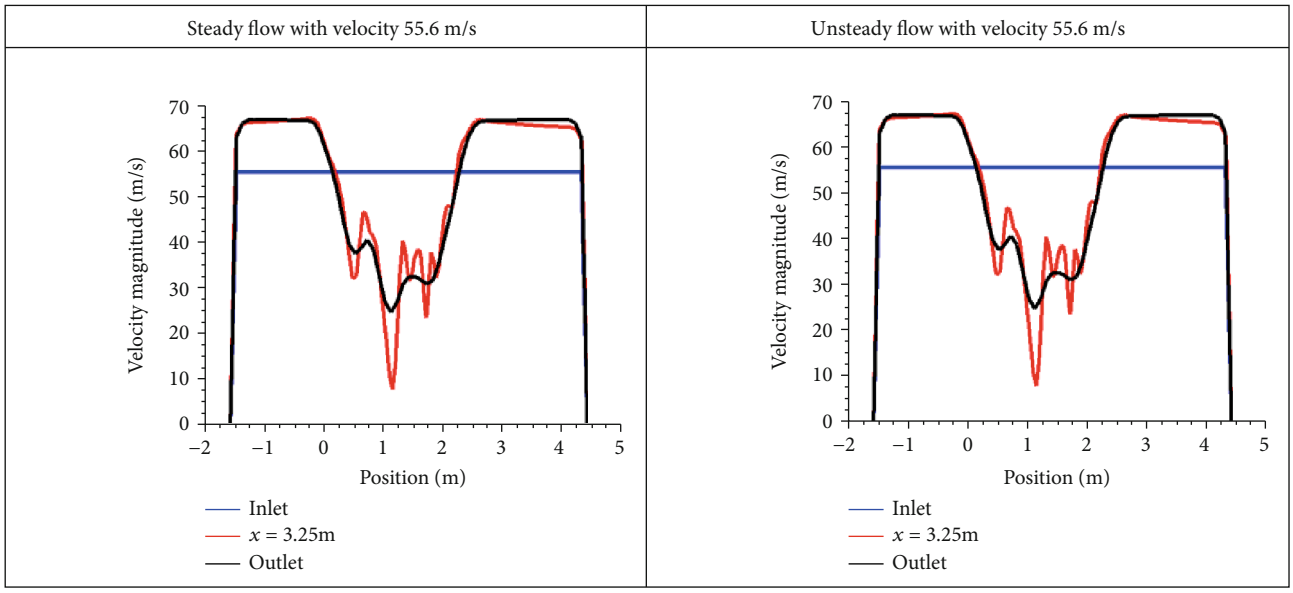

Figure 14: Steady and unsteady velocity dissipation of wind flow at inlet, outlet, and $x = 3.25$ m in case 2.

position. When the velocity of the wind flow is compared at different locations, it can be seen that as the wind flows into the root area, the speed of the wind reduces. However, it should be noted that the speed is near to 0 m/s at various locations. This is due to the interaction of the wind flow with the root edges at the impact point, which results in a stagnation area and a decrease in the velocity of the wind.

The first enlarged root's (far away from the primary trunk) upstream velocities are 11.8 m/s, 26.5 m/s, and 36.0 m/s. In all 3 cases, the downstream velocity is 0 m/s. The perpendicular side red color contour velocities are 42.8 m/s, 90.2 m/s, and 136.1 m/s. The yellow contour velocities are 31.1 m/s, 58.6 m/s, and 90.5 m/s. The light green color contour velocities are 26.3 m/s, 56.1 m/s, and 78.8 m/s in cases 1, 2 and 3 visualized in Figures 3, 10, and 11. The second enlarged image is as follows (near to the primary trunk upstream velocities are 11.8 m/s, 22.5 m/s, and 34.0 m/s. The downstream velocity is 0 m/s in all 3 cases. The velocities of green color contour are 16.7 m/s, 36.1 m/s, and 47.6 m/s in cases 1, 2 and 3, which are visualized in Figures 3, 10, and 11.

The comparison of steady and unsteady pressure distribution of wind flow in cases 1, 2 and 3 is visualized in Figures 10, 11, and 12. The pressure contour of steady and unsteady wind flow in each case is same, which is clearly visualized in these figures. The highest pressure can be observed in the region far away from the stilt roots, which is indicated by red contour. The lowest pressure can be observed near the primary trunk indicated by green contour. The highest pressure in cases 1, 2 and 3 is917.2 Pa, 3609.9 Pa,

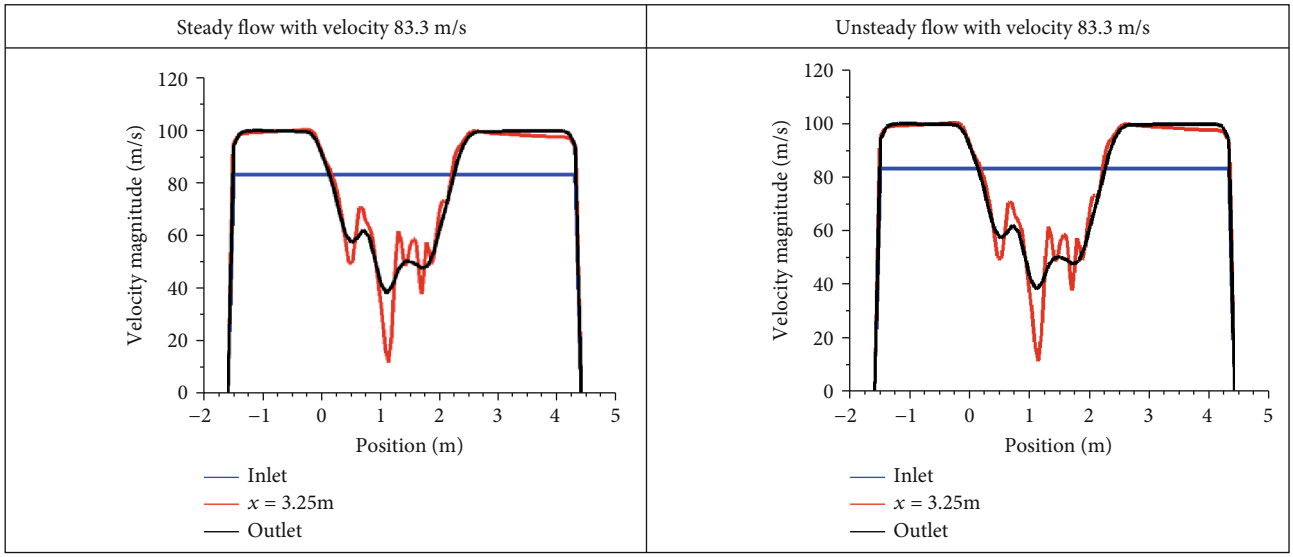

Figure 15: Steady and unsteady velocity dissipation of wind flow at inlet, outlet, and $x = 3.25$ m in case 3.

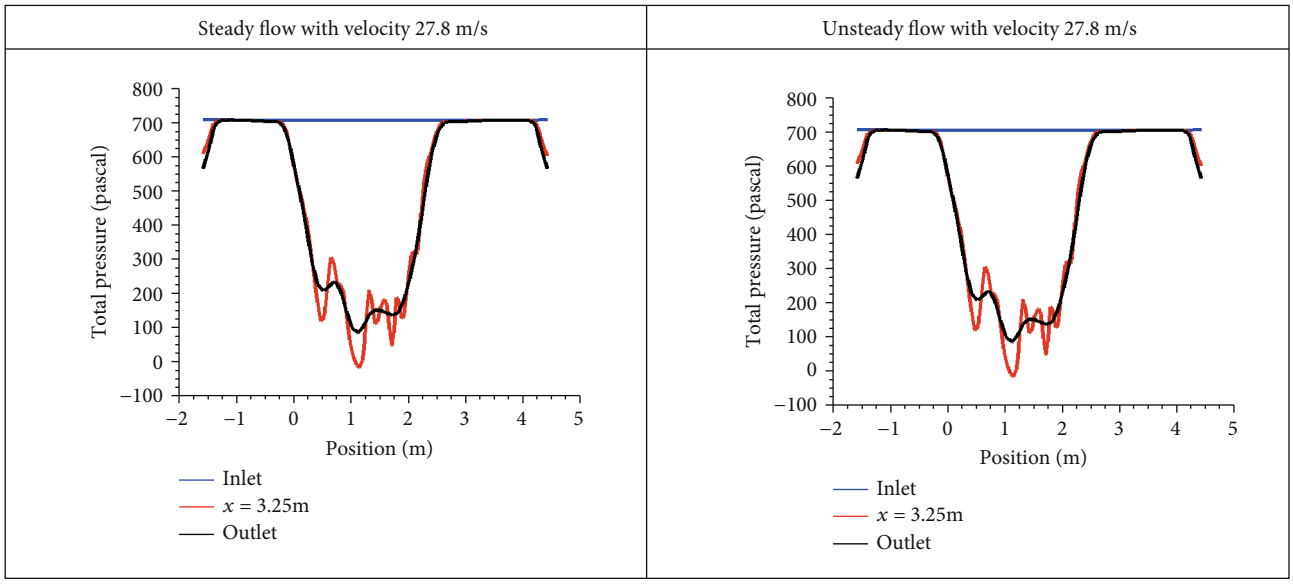

Figure 16: Steady and unsteady pressure variation of wind flow at inlet, outlet, and $x = 3.25$ m in case 1.

and 8017.7 Pa. The first enlarged root's (far away from the primary trunk) downstream green color contour pressures are 74.6 Pa, 457.6 Pa, and 682.6 Pa; downstream yellow color contour velocities are 153.7 Pa, 556.6 Pa, and 682.6 Pa, respectively, in cases 1, 2 and 3. The second enlarge roots' downsteam pressures are -173.5 Pa, -1172.6 Pa, and -1728.8 Pa.

An isosurface is created on the root geometry to compare the velocity reduction. The comparison of steady and unsteady velocity dissipation of wind flow at inlet, outlet, and $x = 3.25$ m in cases 1, 2 and 3 is visualized in Figures 13–15. At the position $x = 3.25$, the velocity decreased up to 88% of the inlet velocity. This position is very near to the primary trunk. To compare the inlet and the outlet velocities also evident that, velocities decrease by more than 50%.

The comparison of steady and unsteady pressure variation of wind flow at inlet, outlet, and $x = 3.25$ m in cases 1, 2 and 3 is visualized in Figures 16, 17, and 18. The position $x = 3.25$ m is very closed to the primary trunk, and the root density is more around this trunk. The pressure variation is clearly observed in these figures, and pressure decreased to below 0 Pascal is clearly observed in these figures.

The result of this study is validated with the previous studies mentioned in the literature and the convergence plots. In each 3 cases, both steady and unsteady cases are converged to 3 decimal place is observed in Figures 4, 5, and 6. Avicenia mangrove roots can reduce the wind velocity

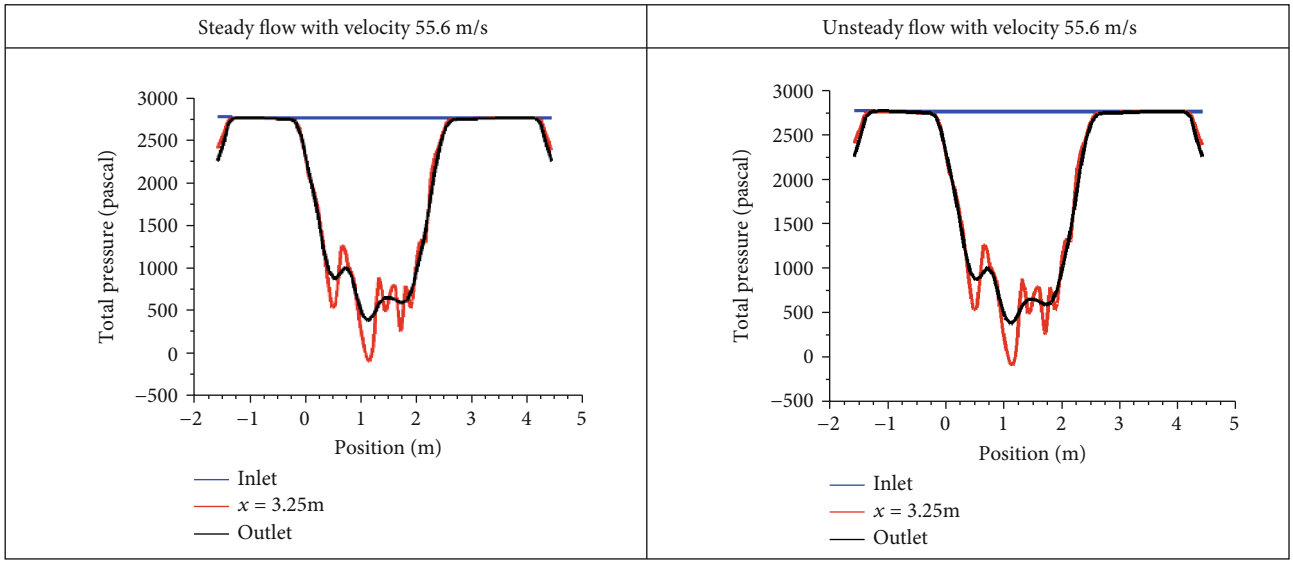

Figure 17: Steady and unsteady pressure variation of wind flow at inlet, outlet, and $x = 3.25$ m in case 2.

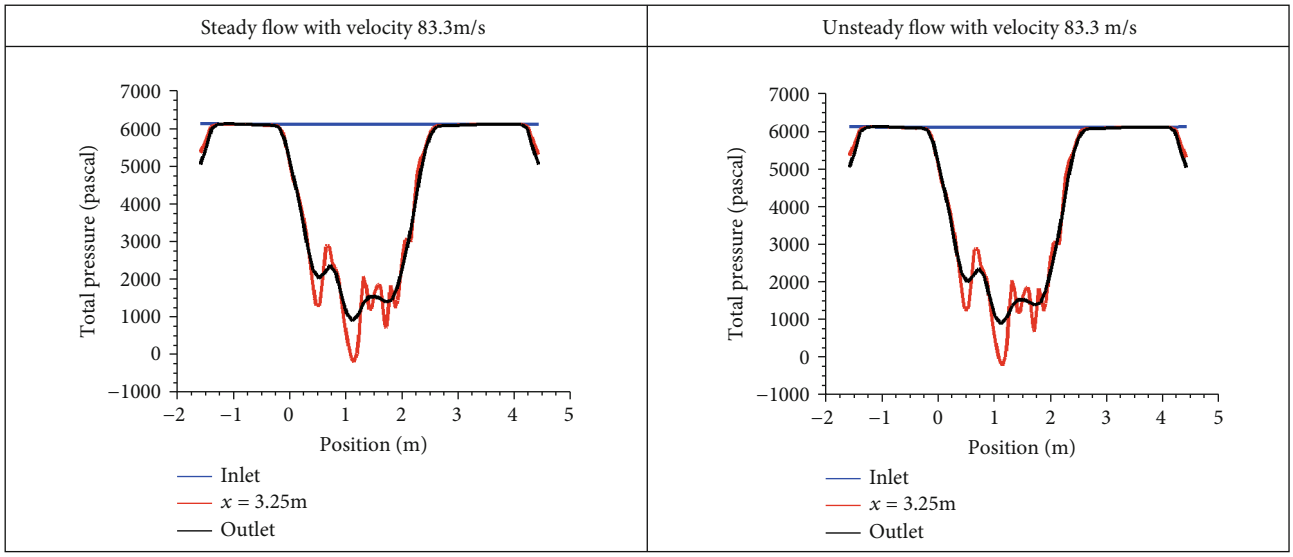

Figure 18: Steady and unsteady pressure variation of wind flow at Inlet, outlet and $x = 3.25$ m in case 3.

to more than 70% according to the study [30]. Rhizophora mangrove root dimensions are more compared to Avicennia mangrove roots, and the structure of the roots is more complex, which is able to reduce more than 80% of wind velocity.

4. Conclusion

In this study, importance of Rhizphora mangrove root structures is examined. The wind flow velocities during the severe tropical storm, the intense tropical cyclonem and the very intense tropical cyclone considered as 100, 200m and 300 km/hr. (steady and unsteady flow) are significantly reduced to more than 80% of the initial velocity because of these root structures. This study also reveals that the speed of the wind reduced to 0 m/s at many places due to the presence of mangrove roots. It is important to avoid over-cutting of Mangrove trees to protect the ecological system from severe and intense tropical storms and cyclones. This study can influence the people to design breakwater models, plant more mangrove trees, and restore the existing ones near the coastal area to protect the villagers staying near the coastal area from natural disasters. In the future, a three-dimensional study will be considered to discuss the subject in a more realistic manner.

Data Availability

The data used to support the findings of this study are included within the article.

Conflicts of Interest

The authors state that the publishing of this work does not include any conflicts of interest.

References

[1] F. Danielsen, M. K. Sørensen, M. F. Olwig et al., "The Asian tsunami: a protective role for coastal vegetation," *Science*, vol. 310, no. 5748, p. 643, 2005.

[2] N. Shuto, "The effectiveness and limit of tsunami control forests," *Coastal Engineering. Japan*, vol. 30, no. 1, pp. 143–153, 1987.

[3] K. Kandasamy and R. Narayanasamy, "Coastal mangrove forests mitigated tsunami," *Estuarine, Coastal and Shelf Science*, vol. 65, no. 3, pp. 601–606, 2005.

[4] Y. Mazda, E. Wolanski, B. King, A. Sase, D. Ohtsuka, and M. Magi, "Drag force due to vegetation in mangrove swamps," *Mangroves and salt marshes*, vol. 1, no. 3, pp. 193–199, 1997.

[5] S. Massel, K. Furukawa, and R. Brinkman, "Surface wave propagation in mangrove forests," *Fluid Dynamics Research*, vol. 24, no. 4, pp. 219–249, 1999.

[6] R. M. Brinkman, *Wave attenuation in mangrove forests: an investigation through field and theo- retical studies*, [Doctoral dissertation] James Cook University, 2006.

[7] P. Vo-Luong and S. Massel, "Energy dissipation in non-uniform mangrove forests of arbitrary depth," *Journal of Marine Systems*, vol. 74, no. 1-2, pp. 603–622, 2008.

[8] C. C. Mei, I. C. Chan, P. L. F. Liu, Z. Huang, and W. Zhang, "Long waves through emergent coastal vegetation," *Journal of Fluid Mechanics*, vol. 687, pp. 461–491, 2011.

[9] H. Behera, S. Das, and T. Sahoo, "Wave propagation through mangrove forests in the presence of a viscoelastic bed," *Wave motion*, vol. 78, pp. 162–175, 2018.

[10] A. Das, S. de, and B. N. Mandal, "Small amplitude water wave propagation through mangrove forests having thin viscoelastic mud layer," *Waves in random and complex media*, pp. 1–18, 2020.

[11] Z. Huang, Y. Yao, S. Y. Sim, and Y. Yao, "Interaction of solitary waves with emergent, rigid vegetation," *Ocean Engineering*, vol. 38, no. 10, pp. 1080–1088, 2011.

[12] G. Ma, J. T. Kirby, S.-F. Su, J. Figlus, and F. Shi, "Numerical study of turbulence and wave damping induced by vegetation canopies," *Coastal Engineering*, vol. 80, pp. 68–78, 2013.

[13] J. Tang, D. Causon, C. Mingham, and L. Qian, "Numerical study of vegetation damping effects on solitary wave run-up using the nonlinear shallow water equations," *Coastal Engineering*, vol. 75, pp. 21–28, 2013.

[14] S. Y. Teh, H. L. Koh, P. L. F. Liu, A. I. M. Ismail, and H. L. Lee, "Analytical and numerical simulation of tsunami mitigation by mangroves in Penang, Malaysia," *Journal of Asian Earth Sciences*, vol. 36, no. 1, pp. 38–46, 2009.

[15] K. Harada and F. Imamura, "Evaluation of tsunami reduction by control forest and possibility of its use for mitigation," in *Proc. of Coastal Engineering*, pp. 341–345, Japan Society of Civil Engineers, 2003, (In Japanese).

[16] T. Suzuki, M. Zijlema, B. Burger, M. C. Meijer, and S. Narayan, "Wave dissipation by vegetation with layer schematization in SWAN," *Coastal Engineering*, vol. 59, no. 1, pp. 64–71, 2012.

[17] F. J. Mendez and I. J. Losada, "An empirical model to estimate the propagation of random breaking and nonbreaking waves over vegetation fields," *Coastal Engineering*, vol. 51, no. 2, pp. 103–118, 2004.

[18] M. Maza, J. L. Lara, and I. J. Losada, "A coupled model of submerged vegetation under oscillatory flow using Navier- Stokes equations," *Coastal Engineering*, vol. 80, pp. 16–34, 2013.

[19] C. C. Mei, I. C. Chan, and L.-F. P. Liu, "Waves of intermediate length through an array of vertical cylinders," *Environmental Fluid Mechanics*, vol. 14, no. 1, pp. 235–261, 2014.

[20] K. Furukawa, E. Wolanski, and H. Mueller, "Currents and sediment transport in mangrove forests," *Estuarine, Coastal and Shelf Science*, vol. 44, no. 3, pp. 301–310, 1997.

[21] S. Hadi, H. Latief, and M. Muliddin, "Analysis of surface wave attenuation in mangrove forests," *Journal of Engineering and Technological Sciences*, vol. 35, no. 2, pp. 89–108, 2003.

[22] Y. Wu, R. A. Falconer, and J. Struve, "Mathematical modelling of tidal currents in mangrove forests," *Environmental Modelling and Software*, vol. 16, no. 1, pp. 19–29, 2001.

[23] S. Y. Lee, J. H. Primavera, F. Dahdouh-Guebas et al., "Ecological role and services of tropical mangrove ecosystems: a reassessment," *Global Ecology And Biogeography*, vol. 23, no. 7, pp. 726–743, 2014.

[24] A. L. McIvor, I. Möller, T. Spencer, and M. Spalding, "Reduction of wind and swell waves by mangroves," in *Natural Coastal Protection Series: Report 1*, Cambridge Coastal Research Unit Working Paper 40, 2012.

[25] N. A. Aziz, O. Inayatullah, M. Jusoh, and M. Z. Bin, "The mechanism of mangrove tree in wave energy propagation," *Advanced Materials Research*, vol. 614-615, pp. 568–572, 2012.

[26] M. Z. M. Jusoh, N. A. Aziz, and O. Inayatullah, "Computational fluid dynamics simulation of flow velocities dissipation by mangrove roots," *ARPN journal of engineering and applied sciences*, 2016.

[27] S. Rahuman, A. M. Ismail, and S. M. Varghese, "Computational fluid dynamic analysis of flow around mangrove roots," *Journal of Physics Conference series*, vol. 1770, no. 1, p. 012052, 2021.

[28] S. Rahuman, M. Ismail, and S. M. Varghese, "Computational fluid dynamic analysis of flow patterns around Rhizophora mangrove roots," *Information and Communication Technology for Competitive Strategies (ICTCS 2020)*, pp. 1111–1120, Springer, Singapore, 2021.

[29] K. Q. Zhang, Y. Liu, X. Hongzhou, S. Jian, J. Rhome, and T. J. SmithIII, "The role of mangroves in attenuating storm surges," *Estuarine, Coatal and Shelf Science*, vol. 102, pp. 11–23, 2012.

[30] S. Rahuman, M. Ismail, and S. M. Varghese, "Computational fluid dynamic analysis of wind flow around mangrove roots to reduce the damage due to heavy wind," *Materials today proceedings*, vol. 44, pp. 3777–3785, 2021.